

Analyses of the Molecular Mechanisms Associated with Silk Production in Silkworm by iTRAQ-Based Proteomics and RNA-Sequencing-Based Transcriptomics

Shaohua Wang,[†] Zhengying You,[†] Mao Feng,[‡] Jiaqian Che,[†] Yuyu Zhang,[†] Qiuji Qian,[†] Setsuko Komatsu,[§] and Boxiong Zhong^{*,†}

[†]College of Animal Sciences, Zhejiang University, Hangzhou 310058, PR China

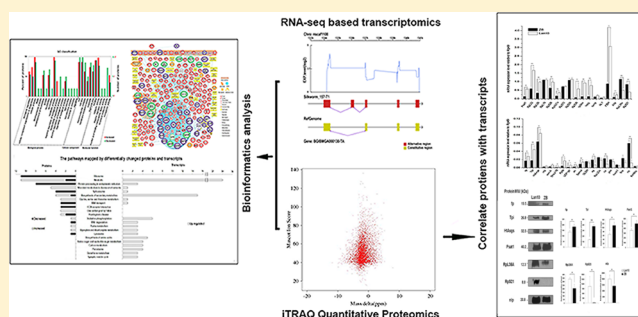
[‡]Institute of Apicultural Research/Key Laboratory of Pollinating Insect Biology, Ministry of Agriculture, Chinese Academy of Agricultural Science, Beijing 100093, China

[§]National Institute of Crop Science, NARO, Tsukuba 305-8518, Japan

Supporting Information

ABSTRACT: Silkworm is used as a model organism to analyze two standard complex traits, which are high and low silk yields. To understand the molecular mechanisms of silk production, the posterior silk glands aged to the third day of the fifth instar were analyzed from the ZB strain with low silk production and from the control strain Lan10. Using isobaric tags for relative and absolute quantification (iTRAQ) quantitative shotgun proteomics and RNA-sequencing-based transcriptomics, 139 proteins and 630 transcripts were identified as novel in the ZB strain compared with the Lan10 strain, indicating that these results significantly expand the coverage of proteins and transcripts of the posterior silk glands in the silkworm. Of the 89 differently changed proteins, 23 were increased, and 66 were decreased. Of the 788 transcripts, 779 were upregulated, and 9 were downregulated. These results confirm that decreased energy utilization/protein translation and enhanced protein degradation are the key factors in lower silk production. Moreover, this study provides novel insight into the molecular changes that may result in lower silk production, namely, a combination of impaired transcription activity, missed protein folding/transport, and lowered yields of the main components of fibroin, along with weakened growth/development of the posterior silk gland.

KEYWORDS: silkworm, complex trait, proteomics, iTRAQ, transcriptomics, silk



INTRODUCTION

The silkworm *Bombyx mori*, which is a holometabolous lepidopteran insect, is the only species that has been fully domesticated by humans for silk production and can be used for scientific research.¹ The silkworm has been used as a lepidopteran model system to investigate the detailed genetic information regarding its morphology, development, and behavior.² The economic importance of the silkworm is its production of fibers composed of silk fibroin. These fibers are produced as high-end materials to fulfill human needs in areas such as industry and medicine (medical sutures).^{3,4} Silk fibroin is usually produced through a spinning and cocooning process. Fibroin and sericin are the major components of the cocoon; fibroin is synthesized by posterior silk glands, is coated with sericin when it goes through the middle silk glands, and then becomes the cocoon after passing through the anterior silk glands.⁵ Normal growth and development of the posterior silk gland is essential for fibroin synthesis.⁶ The cocoon yield is determined primarily by the amount of fibroin secreted from

the posterior silk glands; fibroin consists of three parts: fibroin light chain, fibroin heavy chain, and fibrohexamerin (P25). Ribosomal protein regulation at the translational level is critical for fibroin synthesis,^{7,8} and overexpression of Ras1^{CA}, a mutant oncogene derived from the rat sarcoma protein Ras1^{V12}, in the posterior silk gland improves silk yield.⁹ Silk production by the silkworm is a typical complex trait that is regulated by multiple genes;¹⁰ this production ultimately must manifest as the result of the regulation of proteins, genes, and their pathways.

Silk yield varies among silkworm strains. For strains with high yield on sericulture, 500 mg of silk can typically be obtained from one cocoon, a quantity significantly greater than that of low yielding strains. In particular, the two strains of silkworm “Nd” and “Nd-s” produce extremely small amounts of silk. The reduction in silk production in these two strains is driven by mutations in the fibroin heavy chain¹¹ and fibroin

Received: February 6, 2015

light chain genes,¹² respectively. These mutated strains indicate that the cocoon yield is affected by several biological pathways. A transgenic mutated strain named ZB obtained by our group provided insight into the molecular mechanisms that regulate silk production in silk glands.¹³ The ZB strain has the inherited characteristics of significantly shorter posterior silk glands and extremely low silk production¹³ and provides a good model for investigating the molecular mechanism that regulates silk production in silk glands. It has been reported that the decreased efficiencies of energy utilization and protein translation and the enhanced protein degradation drive the low silk yield in the ZB strain using a gel-free/label-free proteomic technique.¹³

In this study, we applied a proteomic technique, the isobaric tags for relative and absolute quantification (iTRAQ) and an RNA-sequencing-based transcriptome technique in which the transcripts with new exons were identified from an alternative splicing database to further understand the related proteins and transcripts involved in the low silk production in the ZB strain. This study will be helpful developing a comprehensive understanding of how the proteome and transcriptome change in association with physiological changes in silk production.

MATERIALS AND METHODS

Silkworm Rearing and Tissue Isolation

Animal rearing and tissue isolation were performed essentially according to Zhou et al.¹⁴ Briefly, the silkworm strain Lan10 and the mutated strain ZB were raised on fresh mulberry leaves according to our previously described protocol. The samples were dissected on the third day of the fifth instar and frozen in liquid nitrogen for further investigation. Five independent biological individuals were used for proteomic and transcriptomic analyses.

Protein Extraction and Digestion

Protein extraction was performed according to a previously described protocol¹⁵ with minor modifications. In brief, each sample was mechanically homogenized in 300 μ L of lysis buffer containing 7 M urea, 2 M thiourea, 4% 3-[(3-cholamidopropyl)dimethylammonio]propanesulfonate (CHAPS), and 40 mM Tris-HCl (pH 8.5); then, 1 M dithiothreitol (DTT) was added to a final concentration of 10 mM. The supernatant was precipitated in fivefold ice-cold acetone overnight at -20°C . The precipitate was washed with chilled acetone for 30 min, and the supernatant was discarded after centrifugation at 4°C at $25\,000 \times g$ for 20 min. The pellet was air-dried and dissolved in 400 μ L of 0.5 M triethylammonium bicarbonate (TEAB) (Applied Biosystems, Foster City, CA, USA). Then, phenylmethanesulfonyl fluoride and ethylenediaminetetraacetic acid (EDTA) were added to final concentrations of 1 and 2 mM, respectively. After 5 min, DTT was added to a final concentration of 10 mM. The suspension was sonicated at 200 W for 15 min and centrifuged at $25\,000 \times g$ and 4°C for 20 min; then, 10 mM DTT was added to the suspension and incubated for 1 h at 56°C to reduce the disulfide bonds in the supernatant. Cysteine was blocked with 55 mM iodoacetamide and incubated in the dark for 45 min. Thereafter, fivefold chilled acetone was added to the supernatant and incubated at -20°C overnight. The supernatant was discarded after centrifugation at 4°C and $25\,000 \times g$ for 20 min, and the pellet was air-dried for 5 min. The resultant pellet was redissolved in 200 μ L of 0.5 M TEAB, followed by sonication at 200 W for 15 min. The supernatant

was centrifuged at 4°C at $25\,000 \times g$ for 20 min, and the protein concentration was determined using a 2-D Quant Kit (GE Healthcare, Fairfield, CT, USA). The proteins were digested with trypsin (sequencing grade, Promega, Madison, WI, USA) according to the protein/trypsin ratio of 30:1 at 37°C for 16 h.

iTRAQ Analysis

The posterior silk glands from 10 silkworms for each strain were ground for protein isolation. One run was performed for each strain. The trypsin-digested peptides were vacuum-dried, reconstituted in 0.5 M TEAB, and processed according to the manufacturer's protocol for 8-plex iTRAQ labeling (Applied Biosystems). Briefly, one unit of iTRAQ reagent, which is defined as the amount of reagent required to label 100 μ g of protein, was thawed and reconstituted in 70 μ L of isopropanol. Peptides from the transgenic strain ZB and from the control strain Lan10 were labeled with 119 and 121 iTRAQ tags, respectively, by incubation at room temperature for 2 h. Then, the peptide mixtures were pooled and dried by vacuum centrifugation. The iTRAQ-labeled peptide mixture was reconstituted and loaded onto a $4.6 \times 250\text{ mm}^2$ Ultremex SCX (strong cation exchange) column containing 5 μ m particles (Phenomenex, Los Angeles, CA, USA). The peptides were subjected to nanoelectrospray ionization, followed by tandem mass spectrometry (MS/MS) in a TripleTOF 5600 system (AB SCIEX, Framingham, MA, USA). A spray voltage of 2600 V was applied. MS scans were obtained from m/z 400–1800, with 40 precursors selected for MS/MS from m/z 100–2000 using a dynamic exclusion of 30 s for the selected ions. The collision-induced dissociation (CID) energy was automatically adjusted by the rolling CID function of Analyst TF 1.5.1. To prevent the omission of proteins, the database search strategy-based peptide-matching tolerance was controlled below 20 ppm. The error distribution of the relative molecular weight of all the matched peptides is shown in Supporting Information Figure 1. Peptide tolerances and fragment mass tolerances were 20 ppm and 0.02 Da, respectively. Trypsin was used to cleave the peptides, and one missing cleavage site was allowed. A fixed modification of carbamidomethyl at Cys, variable modifications of oxidation at Met, and iTRAQ 8plex at Tyr were specified. iTRAQ 8plex was chosen for simultaneous quantification during the search.

Protein Identification and Quantification

An in-house database was constructed as described previously.¹³ Briefly, the in-house database included the following sequences: the protein sequences of *B. mori* released by the NCBI Refseq, 2123 entries (<http://www.ncbi.nlm.nih.gov/protein?term=txid7091>); the protein sequences of silkworm genes from SilkDB, 14 623 entries (<http://www.silkdb.org/silkdb/doc/download.html>); the protein sequences of *Drosophila melanogaster* downloaded from NCBI, 22 316 entries (<http://www.ncbi.nlm.nih.gov/protein?term=txid7091>); and the foreign protein sequences of EGFP and enterobacteria phage T7 RNA polymerase.¹³ The mgf files were subjected to a search for peptide/protein identification and quantification using the Mascot search engine (version 2.3.0.2, Matrix Science, London, UK). For protein quantification, the peptide for quantification was automatically selected by calculating the reporter peak area using default parameters in the Mascot software package. The resulting data set was corrected for autolysis, and the variations resulting from unequal mixing during the combination of differently labeled samples were

removed. Only proteins with fold changes ≥ 1.5 or ≤ 0.67 and with $P < 0.05$ (using one-way ANOVA) were considered significantly changed levels of increase or decrease between the strains ZB and Lan10. The false discovery rate (FDR) was controlled using a target/decoy database method for peptide/protein identification with a cutoff score of 20.0 ($FDR \leq 1.0\%$).

Western Blot Analysis

Western blotting was performed to validate the protein abundance in both ZB and Lan10. The polyclonal antibodies were prepared by GenScript (Piscataway, NJ, USA). The target sites for the seven proteins fp, Tpi, HtAsgs, Past1, RpL36A, RpS21, and nlp were CQYKQQRDLGKAST, GGNW-KMNGDKNQINC, CIRNRLSEPGAENIK, FGAGP-AKLPEEVYEC, CRYDRKQQGYGGQSK, CDVDPATGRA-ADTSK, and CAKGKAASPKNAKK, respectively. The first antibodies were obtained from New Zealand rabbits. Goat anti-rabbit IgG conjugated with horseradish peroxidase (Bio-Rad, Hercules, CA, USA) served as the secondary antibody. The posterior silk glands from the silkworm strains ZB and Lan10 were ground to powder in liquid nitrogen. Three biologically independent individuals were used. The 100 μL of lysates consisted of 1% Triton X-100, 1% sodium deoxycholate, and 0.1% SDS added to each 10 mg of tissue to crack and degrade the posterior silk glands. The resulting solution was centrifuged at $15\,000 \times g$ at 4°C for 10 min. The supernatant was collected and the protein concentration was measured using BCA methods.¹⁶ The proteins were separated by gel separation using 10, 12, and 15% polyacrylamide according to the molecular weight of the proteins. The quantity of the loading sample was 50 μg . Actin 3 was used as reference protein to calibrate the quantity of the loading sample. The relative intensities of bands were calculated by ImageJ software.

Transcriptomic Analysis

RNA sequencing was performed according to the previous study.¹³ There were 5 028 800 perfect mapped reads for Lan10 and 6 875 343 for ZB. The 9850 genes differ by more than twofold of their transcripts abundance. For analysis, the alternatively spliced genes were filtered according to the criterion that the RPKM (reads per kilobase of exon model per million mapped reads) values of the transcript in the ZB or Lan10 strains should be more than 100. Compared with Lan10, the alternatively spliced genes with changes ≥ 2 -fold or ≤ 0.5 -fold in the ZB strain were defined as upregulated and downregulated, respectively. The posterior silk gland transcripts with new exons between the strains ZB and Lan10 were obtained by comparing these transcripts to the gene and genome databases. The gene database was compiled from the following four resources: (1) 14 623 silkworm gene sequences downloaded from <http://www.silkdb.org/silkdb>, (2) 11 104 silkworm genes with complete cDNA sequences downloaded from <http://sgp.dna.affrc.go.jp/FLcDNA/>, (3) 13 952 silkworm gene sequences downloaded from NCBI <http://www.ncbi.nlm.nih.gov> (txid7091), and (4) 17 127 *Drosophila* gene sequences downloaded from NCBI <http://www.ncbi.nlm.nih.gov> (txid7227). The gene database was constructed on the basis of resource 1 and combined with resources 2–4 in turn with no redundancy. The silkworm genome database was downloaded from <http://www.silkdb.org/silkdb>. The transcript sequencing results were searched on the basis of the gene and genome databases to obtain the alternatively spliced genes. The alternatively spliced genes were filtered according to the criterion that a RPKM values of the

transcript in the ZB or Lan10 strains should be more than 100. Compared with Lan10, the alternatively spliced genes with fold changes ≥ 2 or ≤ 0.5 in the ZB strain were defined as up- or downregulated, respectively.

qRT-PCR Analysis

Total RNA from each sample was isolated using TRIzol reagent (Invitrogen, Carlsbad, CA, USA) according to the manufacturer's instructions. Three independent biological replicates were performed for each silkworm strain. Total RNA integrity was determined by gel electrophoresis, and the RNA concentration was measured by absorbance at 260 and 280 nm ($1.9 < A_{260/280} < 2.1$). The resultant RNA was reverse-transcribed for cDNA synthesis using a PrimeScript RT Reagent Kit with gDNA Eraser (TaKaRa, Osaka, Japan). qRT-PCR was performed in a 20 μL reaction system with 50 ng of reverse transcription product, 40 nM each of the forward and reverse primers, and the SYBR Premix Taq (TaKaRa). Rox Reference Dye I and a 7500 real-time PCR system were used (Applied Biosystems). The running program began at 95°C for 30 s for activation, followed by 40 cycles of amplification at 95°C for 5 s and 58°C for 30 s. Then, an additional 15 s at 95°C , 1 min at 60°C , and 15 s at 95°C were performed for the melt curve stage. The transcript expression level was calculated on the basis of the delta Ct value, which was normalized to that of the reference gene RP49 (accession no. NM_001098282) according to the $R = 2^{-\Delta\Delta\text{Ct}}$ method. The Student's *t* test was used in the statistical analysis. The gene-specific primers (Supporting Information Table 1) were designed using Beacon Designer 7 (Premier Biosoft International, Palo Alto, CA, USA).

Bioinformatic Analysis

The sequences of the differentially expressed proteins were subjected to a BLAST query against the GO database (<http://www.geneontology.org/>). The corresponding GO terms were extracted from the most homologous proteins using a Perl program. The GO annotation results were plotted using the Web Gene Ontology Annotation Plot (WEGO) (<http://wego.genomics.org.cn/cgi-bin/wego/index.pl>) tool by uploading the compiled WEGO native format files containing the obtained GO terms.¹⁷ The functional classification of proteins was performed according to <http://www.uniprot.org/>. BIN was built using Pathway Studio software (version 8.0, Ariadne Genomics, Rockville, MD, USA). The protein IDs of *D. melanogaster* homologies were retrieved from the *Drosophila* database (version 1.0, released on December 1, 2008) and contained the relationships of protein interaction data published in the literature.¹⁸ The interactions were filtered out when the number of references was less than or equal to 2. The FASTA files of protein sequences of differentially changed proteins were searched against the online KEGG database (<http://www.genome.jp/tools/blast/>),¹⁹ and the corresponding KEGG pathways that these proteins were mapped to were extracted.

RESULTS

Changes in Protein Abundance between ZB and Lan10

The posterior silk gland is a primary organ that is responsible for the synthesis and secretion of the silk protein, and the third day of the fifth instar of this organ is a critical time window for the production of a large amount of silk.⁷ In an effort to extend proteome coverage and knowledge regarding how the

Table 1. Differentially Changed Proteins Identified by iTRAQ from the Posterior Silk Gland of the Silkworm on the Third Day of the Fifth Instar

accession ^{a,b}	description	score ^c	mass	cov ^d	unique spectrum ^e	unique peptide ^f	fold change (ZB/Lan10)
Increased							
gi_1377915	enhanced green fluorescent protein (EGFP)	318	35855	14.7	28	4	8.93
BGIBMGA008768	ferritin precursor	172	23887	12.7	8	2	2.69
BGIBMGA006056	probable H/ACA ribonucleoprotein complex subunit 1	37	25888	11.6	2	2	2.06
gi_187281708	triosephosphate isomerase	236	33017	12.9	4	2	1.89
BGIBMGA002689	seroin 1 precursor	360	10081	53.5	19	3	1.86
BGIBMGA014201	cytosolic 10-formyltetrahydrofolate dehydrogenase-like	739	80557	27.2	36	12	1.68
BGIBMGA013965	H+-transporting ATP synthase gamma subunit	184	39192	8.4	6	2	1.53
gi_114052677	phosphoserine aminotransferase 1	815	49167	31.3	31	9	1.51
gi_114051239	cystathionine gamma-lyase	807	51332	15	28	5	2.36
BGIBMGA009647	histone H2A-like isoform X3	875	15055	47.6	51	5	2.35
gi_114052645	thymosin isoform 1	167	26172	26.5	13	4	2.03
BGIBMGA002355	NAD-dependent methylenetetrahydrofolate dehydrogenase	145	39081	19.6	11	5	1.97
BGIBMGA012309	D-3-phosphoglycerate dehydrogenase-like	447	56800	19.7	22	8	1.81
BGIBMGA007072	yellow-b	98	55547	6.7	8	3	1.75
BGIBMGA012839	cytosolic 10-formyltetrahydrofolate dehydrogenase	138	13200	45.1	9	3	1.72
BGIBMGA000672	probable citrate synthase 1, mitochondrial-like	374	63313	13.5	13	5	1.71
BGIBMGA011337	regucalcin	273	41486	9.8	8	2	1.71
BGIBMGA001037	leucine-tRNA ligase, cytoplasmic-like	152	172733	4.3	10	4	1.7
BGIBMGA004776	arg methyltransferase	448	50222	11.9	11	3	1.66
BGIBMGA007631	nucleolar complex protein 4 homologue B-like	73	62268	4.8	3	2	1.64
BGIBMGA014563	lysine-specific demethylase	124	75602	9.6	11	4	1.58
BGIBMGA003330	probable uridine nucleosidase 2-like	55	40827	10	3	2	1.58
BGIBMGA003001	nucleolar complex protein 2 homologue	105	97010	4	4	2	1.5
Decreased							
BGIBMGA004374	ribosomal protein S12	577	20234	46	32	5	0.62
BGIBMGA006789	malectin-like	183	36065	17	11	4	0.61
BGIBMGA002565	unknown secreted protein	119	30689	12.9	3	2	0.42
BGIBMGA002626	antennal binding protein precursor	75	20871	15.3	3	2	0.36
BGIBMGA001353	protein ERGIC-53-like	167	36823	12.5	5	2	0.67
BGIBMGA010289	UDP-glucosyltransferase precursor	193	131233	5.4	15	4	0.67
BGIBMGA007844	surfeit locus protein 6 homologue	65	44664	9.4	5	2	0.66
BGIBMGA005635	Sr protein	744	22305	12.8	25	3	0.66
BGIBMGA006405	heterogeneous nuclear ribonucleoprotein A2/B1	133	47238	7.2	5	2	0.66
BGIBMGA006986	ribosomal protein L22	179	24464	29.9	14	3	0.66
BGIBMGA012032	10 kDa heat shock protein, mitochondrial	92	14528	21.4	4	2	0.66
BGIBMGA001265	eukaryotic translation initiation factor 5B, partial	181	182590	7.8	11	6	0.65
BGIBMGA010595	hsc70-interacting protein-like isoform X1	94	53233	7.1	4	2	0.65
BGIBMGA011004	DDRGK domain-containing protein 1 precursor	120	42462	17	7	3	0.65
BGIBMGA012944	fatty acid binding protein	77	19569	13.6	6	2	0.65
gi_256773186	sarco/endoplasmic reticulum calcium ATPase	508	132850	14.7	28	12	0.64
BGIBMGA010839	vesicular mannose-binding lectin-like protein	100	44438	7.2	4	2	0.64
BGIBMGA000206	fibrillin-1-like	1567	54044	25.4	43	7	0.64
BGIBMGA006856	notch-like protein	397	2364543	0.7	21	9	0.63
BGIBMGA010164	hypothetical protein	138	57641	6.1	6	2	0.63
BGIBMGA010970	ribosomal protein L26	77	24145	14.2	8	2	0.63
BGIBMGA011651	anamorsin homologue	331	36506	10.8	7	2	0.62
BGIBMGA004992	adipocyte plasma membrane-associated protein-like	410	101810	6.7	17	3	0.62
BGIBMGA006523	glucosidase II beta-subunit	72	53138	4.5	6	2	0.61
BGIBMGA007363	ribosomal protein S26	133	18094	20.9	13	2	0.6
gi_114051930	prefoldin beta subunit	152	21045	25.4	9	3	0.6
BGIBMGA006932	NECAP-like protein	422	23324	17.1	12	2	0.6
BGIBMGA008954	zinc finger CCHC domain-containing protein 9-like	63	72601	7.2	4	2	0.6
BGIBMGA009189	prefoldin subunit 2	319	19982	30.1	13	3	0.6
BGIBMGA002309	nucleoplasmin-like protein	91	27219	18.7	5	2	0.6
BGIBMGA006209	transport protein Sec61 beta subunit	206	11636	36.1	15	3	0.6
BGIBMGA011446	ribosomal protein S30	72	18355	8.5	10	2	0.59

Table 1. continued

accession ^{a,b}	description	score ^c	mass	cov ^d	unique spectrum ^e	unique peptide ^f	fold change (ZB/Lan10)
		Decreased					
BGIBMGA012905	RAN binding protein	87	33039	9.1	4	2	0.58
BGIBMGA006779	probable protein phosphatase CG10417-like	88	86475	7.6	5	3	0.58
BGIBMGA009967	DnaJ-19	207	107976	6.4	13	4	0.57
BGIBMGA011273	ubiquitin and ribosomal protein S27a	2830	31996	27	52	2	0.57
BGIBMGA001060	clathrin light chain	865	28842	11.4	25	2	0.57
BGIBMGA004059	peptidylprolyl isomerase B precursor	52	28572	22	5	4	0.57
BGIBMGA010475	dynein heavy chain 2, axonemal-like	822	454880	4.1	46	12	0.57
BGIBMGA007822	heterogeneous nuclear ribonucleoprotein A1	175	34911	9	11	2	0.57
BGIBMGA010487	ribosomal protein L36A	129	19930	20.2	11	3	0.56
BGIBMGA000207	fibrillin-1-like	978	68825	8.3	27	3	0.56
BGIBMGA012239	hypothetical protein	80	46471	8.7	6	3	0.56
BGIBMGA006976	BAG domain-containing protein Samui	64	94222	7.3	6	4	0.56
BGIBMGA000475	calreticulin precursor	538	61004	28.4	28	8	0.55
BGIBMGA000505	hypothetical protein AaeL_	124	18004	25	5	2	0.55
BGIBMGA010993	tubulin-folding cofactor B-like isoform X1	34	22862	9.5	2	2	0.54
BGIBMGA005323	ALY	396	33034	35.4	21	7	0.54
BGIBMGA004675	uncharacterized protein	223	160759	2.4	5	2	0.53
gi_164448672	silk fibroin heavy chain	2162	395607	1.1	85	6	0.53
BGIBMGA005559	mesencephalic astrocyte-derived neurotrophic factor	133	29192	19.7	9	3	0.52
BGIBMGA002572	ribosomal protein L19	409	38440	22.6	30	6	0.5
BGIBMGA006835	ribosomal protein L23A	271	56099	12.3	23	5	0.49
BGIBMGA002713	ATPase inhibitor-like protein	194	19104	27.5	15	5	0.48
BGIBMGA011948	40S ribosomal protein S28	440	8892	32.3	29	2	0.48
BGIBMGA012030	unknown unsecreted protein	99	60364	16.8	5	4	0.48
BGIBMGA014039	collagen, type IV	260	234458	4.3	18	6	0.48
BGIBMGA001363	40S ribosomal protein S21	365	11163	34.6	34	2	0.47
BGIBMGA007639	surfeit 4-like protein	77	31640	9	3	2	0.46
BGIBMGA002549	cuticular protein RR-1 motif 5 precursor	261	17746	16	10	2	0.46
BGIBMGA007604	hypothetical protein	739	141559	4.4	25	3	0.46
BGIBMGA005372	LDLR chaperone boca	386	27501	36.4	17	5	0.46
BGIBMGA005328	translocon-associated protein gamma isoform 1	196	24780	8.8	16	2	0.42
BGIBMGA003718	translocation associated membrane protein	115	51670	7.4	5	2	0.4
BGIBMGA014040	collagen alpha-1(IV) chain	285	207513	1.4	12	2	0.38

^aAll the BGIBMGAxxxxxx_PA were written as BGIBMGAxxxxxx. ^bBold accession number indicates that the differentially changed proteins overlapped with the previous study.¹³ ^cScore for protein identification. ^dOverlap ratio of the protein sequence. ^eUnique spectrum mapped on the protein. ^fUnique peptide mapped on the protein.

proteome changes to drive silk production, high-sequencing-speed, mass-accurate MS- and iTRAQ-based proteomics were applied to identify and analyze the differences in protein expression between the posterior silk glands of the strain ZB (which is a genetic mutant strain with low silk production) and the control strain Lan10 at the third day of the fifth instar. Of the 1106 identified proteins, 89 quantifiable proteins with more than 2 unique peptides were significantly changed between ZB and Lan10 (Supporting Information Table 2), with 24 displaying increased abundance levels, and 65 displaying decreased abundance levels (Table 1).

Of the 24 proteins with increased expression levels, 7 of them participated in energy metabolism, including H⁺-transporting ATP synthase gamma subunit, dihydrolipoamide dehydrogenase, citrate synthase 1, D-3-phosphoglycerate dehydrogenase, triosephosphate isomerase, ATPase inhibitor-like protein, and ferritin precursor. In addition, NAD-dependent methylenetetrahydrofolate dehydrogenase and cytosolic 10-formyltetrahydrofolate dehydrogenase were identified, both of which are involved in folate metabolism. Of the 65 proteins with reduced levels of abundance, the major protein type represented was ribosomal proteins (11; 16.9% of 65) related to protein

synthesis and secretion, including 6 ribosomal small subunit-related proteins, i.e., RPS12, PRS21, RPS26, RPS27a, RPS28, and RPS30, and 5 ribosomal large subunit-related proteins, i.e., RPL19, RPL22, RPL23A, RPL26, and RPL36A. Four proteins were associated with the process of peptide/protein transportation to the ER and Golgi, including transport protein Sec61 beta subunit, DnaJ-19 (Translocation protein Sec63 homologue), translocon-associated protein (TRAP) gamma isoform 1, and translocation-associated membrane (TRAM) protein. Two proteins, sarco/ER calcium ATPase and calreticulin precursor, were related to Ca²⁺ transport involved in protein transportation. Five proteins, eukaryotic translation initiation factor 5B, heterogeneous nuclear ribonucleoprotein A2/B1 homologue, heterogeneous nuclear ribonucleoprotein A1, Sr protein, and ALY, were identified as being associated with transcriptional activity. Three proteins with decreased levels of abundance were implicated in protein folding, including prefoldin beta subunit, DnaJ-19, and peptidylprolyl isomerase B precursor. Four proteins showing decreased abundance were associated with the growth and development of cells, i.e., UDP-glucosyltransferase precursor, anamorsin homologue, the BAG domain-containing protein Samui, and

notch-like protein. In addition, fibroin heavy chain, which is the primary component of fibroin, showed decreased abundance.

Compared with our previous study,¹³ of the significantly changed expressed proteins identified by iTRAQ labeling quantification 86.5% (77 proteins) were identified as novel proteins, and only 13.5% (12 proteins) overlapped with label-free quantification (Table 1, bold accession numbers). These novel, differentially expressed proteins enabled us to explore the molecular mechanism of silk production on the basis of additional information. The differentially expressed proteins that overlapped with the label-free quantification were also essential to the illustration of the molecular mechanism underlying silk production. In particular, of those overlapped proteins with increased abundance, five were associated with energy metabolism, confirming the inefficient energy application in the ZB strain compared with Lan10.

GO Analysis of Differentially Changed Proteins

Regarding the GO term assignments of the 89 differentially expressed proteins (Figure 1) associated with the biological

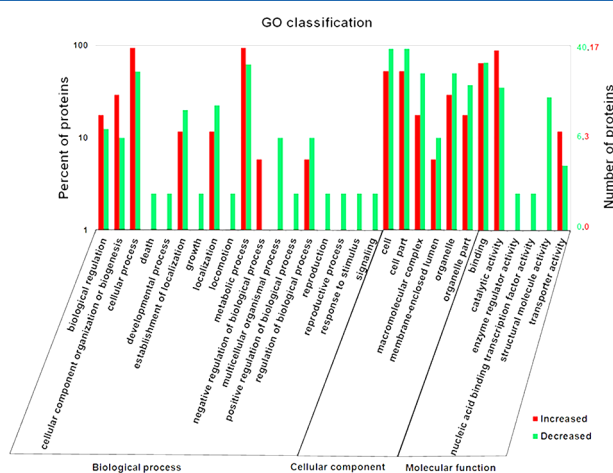


Figure 1. GO categories of proteins with differential abundance between ZB and Lan10. Proteins identified by iTRAQ with differential abundances were classified by biological process, cellular component, and molecular function by WEGO according to the GO terms. The number of proteins mapped to the GO terms is shown in the right panel. The percentages of increased (red) and decreased (green) proteins mapped to the GO terms are shown in the left panel.

process category, the unique terms that matched the proteins with decreased abundance were death, developmental process, growth, locomotion, multicellular organismal process, positive regulation of biological process, reproduction, reproductive process, response to stimulus, and signaling. The unique term that matched the proteins with increased abundance was negative regulation of biological processes. Proteins with decreased abundance were highly represented in three terms: establishment of localization, localization, and regulation of biological process. The proteins with increased abundance were highly represented in four terms: biological regulation, cellular component organization or biogenesis, cellular process, and metabolic process. For the cellular component category, the proteins with lower abundance were more highly represented in this category than proteins with higher abundance in all the terms, and 21 proteins were localized to the micromolecular complex, of which almost half were ribosomal proteins. For molecular function, the proteins with higher abundance

involved in catalytic activity were more highly represented than the proteins with lower abundance. The unique terms annotated to the proteins with decreased abundance were enzyme regulator activity, nucleic acid binding transcription factor activity, and structural molecular activity.

BIN Analysis of Differentially Abundant Proteins

The functions of proteins are determined depending on the interactions found in the biological network. System-wide BIN analysis provides a comprehensive understanding of which proteins play key roles in a certain process, such as modulating silk yield. Of the 89 differentially abundant proteins, 49 were highly networked in the BIN as key node proteins, of which 13 had increased abundance and 36 had decreased abundance (Supporting Information Figure 2 and Supporting Information Table 3). Of the 15 proteins with decreased abundance in the nucleus, 9 were ribosomal proteins, including rpl23a and rps21, with interaction degrees of 13 and 20, respectively, and 3 proteins had nucleotide binding activity, including aly, hrb98de, and nlp. These proteins interacted with a large number of transcription factors in the BIN to regulate cell metabolism. For instance, nlp interacted with nine other proteins in the network. Seven proteins with decreased abundance in the ER, i.e., CG11642, CG6453, spo, crc, boca, surf4, and ca-p60a, were linked in the BIN. Three low-level abundance proteins were linked to the mitochondria, including cg11267, l(2)tid, and hrb27c. However, three other highly abundant proteins in the BIN were related to energy metabolism, i.e., atpsyn-gamma, cg7430, and aldh-iii. Three proteins with decreased abundance that were enriched in the plasma membrane were functionally related cell membrane proteins, i.e., cg25c, sec61 beta, and clc.

Differentially Changed Transcripts between ZB and Lan10

To detect the differences in transcript expression between ZB and Lan10, transcripts with new exons were examined in this study. Interestingly, many transcripts with new exons were obtained by comparing the P50 silkworm strain with the ZB and Lan10 strains; however, the expression levels of these transcripts were different between ZB and Lan10. Of the 788 differentially changed transcripts between strains ZB and Lan10, 779 and 9 were upregulated and downregulated, respectively (Supporting Information Table 4). A large number of upregulated transcripts were related to energy metabolism, including acetyl-coenzyme A synthetase, ATPase subunit β , γ , C, S1, catalase, glucose dehydrogenase, and acyl-CoA dehydrogenase family member 9. Some upregulated transcripts were associated with proteolysis, including aminoacylase-1, furin-like protease 2, aminopeptidase N, serine protease, trypsin, alkaline A, carboxypeptidase A2, and collagenase. Among these transcripts is apoptosis-inducing factor, which is localized to mitochondria and mediates caspase-independent cell death.²⁰ Only 9 of 788 transcripts were downregulated. Of these nine, five were annotated in insects, including pseudoobscura, slimb, probable cytochrome P450 4d20, LIM-binding protein, and ionotropic kainate 5, and four were without annotations. Of the 788 transcripts in this study, only 158 were found in the transcript data set of a previous study, indicating that the databases used in the two studies yield complementary results.

GO Analysis of Differentially Changed Transcripts

Of the 788 transcripts, none of the down-regulated genes were mapped to GO terms (Supporting Information Table 5). Overall, the genes that were upregulated at the transcriptional

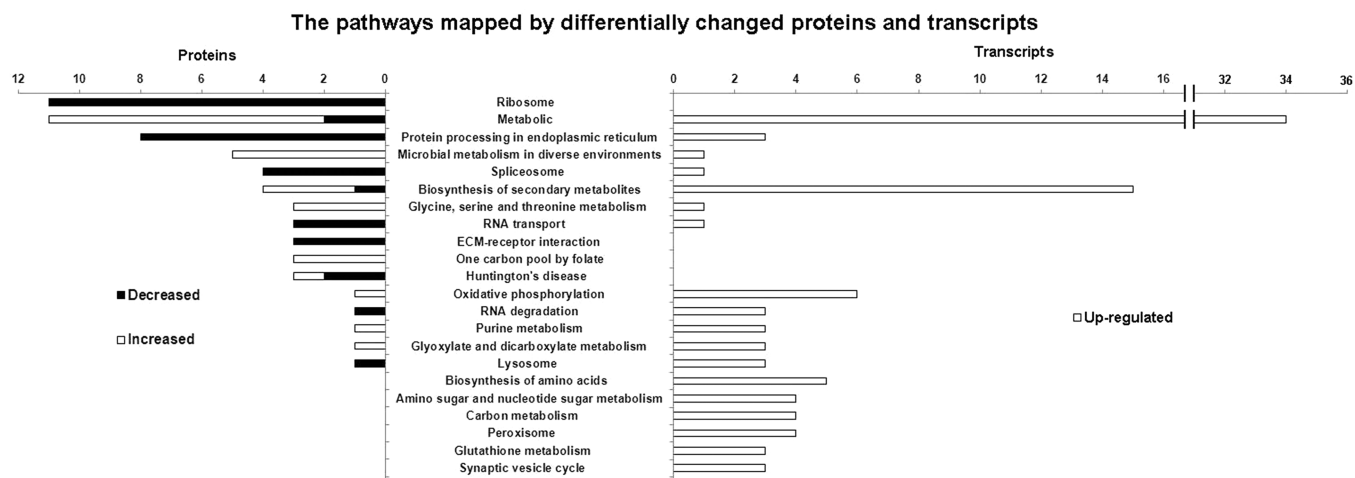


Figure 2. Enriched KEGG pathways of differentially altered proteins and transcripts between ZB and Lan10. The top panel shows the number of proteins and transcripts mapped to the pathway. The white bars represent the enriched pathway of increased/upregulated proteins/transcripts, and the black bars represent the enriched pathway of decreased/downregulated proteins/transcripts.

level were associated with GO terms. In the biological process category, energy metabolism, including metabolic process, carbohydrate metabolic process, and oxidation–reduction, were the most represented terms. Proteolysis was the second most enriched term, indicating that protein degradation is more active in the ZB strain. Transmembrane transport was also highly represented but was involved primarily in proteins for the transport of specific substances, such as transporter for monocarboxylate, sugar, synaptic vesicular amine, organic cation, inorganic phosphate, and cationic amino acid. In contrast, proteins related to transportation functions had decreased abundance levels, indicating that the metabolic activity in the ZB strain was enhanced; however, the activity of cell transportation was impaired. In addition, 20 transcripts were associated with transcriptional regulation. In the cellular component category, the upregulated transcripts were involved primarily in membrane, intracellular, nucleus, integral to membrane, cytoplasm, extracellular region, plasma membrane, cytoskeleton, and mediator complex involved in most parts of a cell. In the molecular function category, the most represented term was protein binding. The terms related to energy metabolism were ATP binding, catalytic activity, oxidoreductase activity, and GTP binding, which were generally consistent with the proteome results. In addition, nucleic acid binding was also highly represented. In general, a similar coverage of GO terms was annotated between the proteome and transcriptome.

Pathway Analysis of Differentially Changed Proteins and Transcripts

The differentially changed proteins and transcripts between the ZB and Lan10 strains were subjected to KEGG pathway analysis (Figure 2 and Supporting Information Table 6). Of the proteins showing decreased abundance, the ribosome, protein processing in ER, spliceosome, and RNA transport pathways were significantly enriched. The proteins showing increased abundance were significantly enriched in the pathways of metabolic and microbial metabolism in diverse environments. However, the downregulated transcripts could not be mapped to any pathways. Sixty percent of the pathways represented by enriched proteins and transcripts overlapped. In the pathways mapped by upregulated transcripts, the metabolic pathway had the highest representation, which was in accordance with the protein pathways, indicating increased metabolism in the ZB

strain. Notably, 15 upregulated transcripts were mapped to the biosynthesis pathway of secondary metabolites, which is involved in energy metabolism in organisms.²¹ Another energy-metabolism-related pathway, oxidative phosphorylation,²² was also highly enriched.

Correlation between mRNA Expression and Protein Abundance

To examine the tendencies between the protein and mRNA expression trends, qRT-PCR was applied to examine the transcript levels of selected proteins in the ZB strain. Thirty-six protein-synthesis- and -secretion-related proteins were selected. These proteins were involved in energy metabolism, ribosome assembly and function, protein folding, processing and transport, posterior silk gland growth and development, and fibroin heavy chain, the major component of fibroin (Supporting Information Figure 3 and Supporting Information Table 8). The expression levels of 23 of 36 genes were significantly altered (fold change >1.5 or <0.67 and $P < 0.05$) in the ZB strain relative to those of the Lan10 strain at the transcriptional level (Figure 3 and Supporting Information Table 7). Of the 23 genes that were significantly altered at the mRNA level, 16 were regulated in the same trend as their corresponding proteins (Figure 4 and Supporting Information Table 7). Among the energy metabolism-related genes, one displayed a consistent trend between mRNA and protein expression. For 18 genes whose protein abundances decreased in the ZB strain relative to the Lan10 strain, 15 also displayed decreased mRNA levels. The genes related to ribosome and protein transport showed lower expression levels in the posterior silk glands, particularly one of the fibroin components, fibroin heavy chain. These results showed that the expression levels of genes related to ribosome function, protein folding, processing, and transport, posterior silk gland growth and development, and fibroin complex are reduced at both transcriptional and translational levels in the ZB strain.

Confirmation of Proteins Abundance

Seven proteins that were up- or downregulated on the basis of the corresponding transcripts were chosen for the Western blot analysis (Figure 5 and Supporting Information Table 7). In the ZB strain, four proteins that the proteomic analysis revealed as related to energy metabolism were present at higher intensities

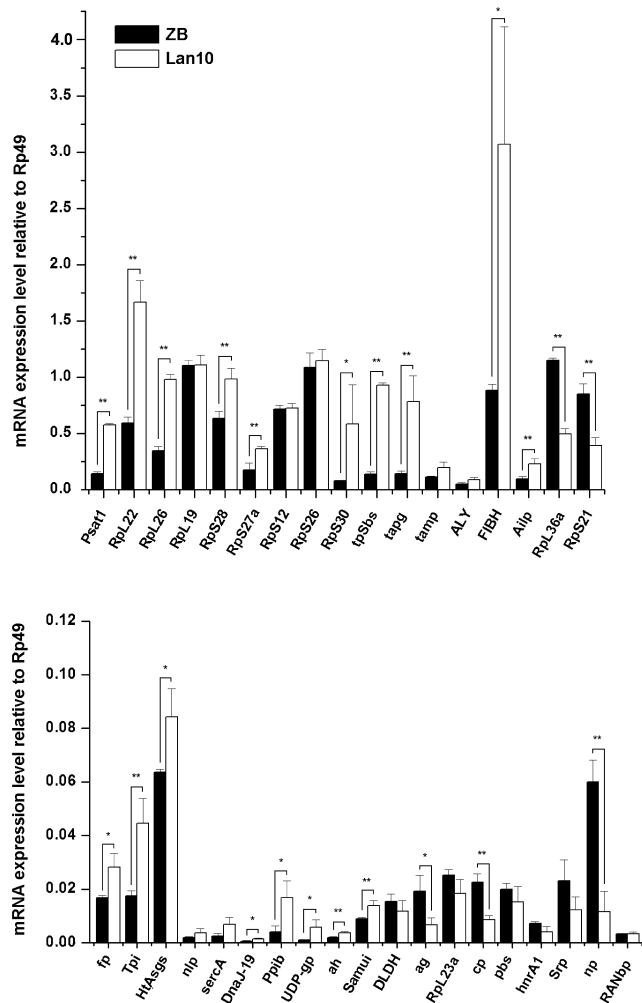


Figure 3. qRT-PCR qualification of differentially altered proteins involved in protein synthesis and secretion between ZB and Lan10. ** indicates that the difference in gene expression between ZB and Lan10 reached the extremely significant level, $P < 0.01$, and * indicates that the difference in gene expression between ZB and Lan10 reached a significant level, $0.01 < P < 0.05$.

in Western blot validation compared to those in Lan10. They were ferritin precursor, triosephosphate isomerase, the H^+ -transporting ATP synthase gamma subunit, and phosphoserine aminotransferase 1. Three proteins whose expression decreased in the ZB strain, ribosomal protein L36A, ribosomal protein S21, and nucleoplasmin-like protein, were recorded at lower intensities relative to those in Lan10 in the Western blotting experiment. Further analysis of the Western blot indicated that the proteomic analysis was credible.

Relationship between the Differentially Changed Proteins/Transcripts and Silk Production

A comprehensive view of the molecular mechanism underlying silk production was summarized on the basis of the results of the current and previous studies (Figure 6 and Supporting Information Table 7). The five aspects proposed to relate to regulation were energy metabolism, transcription/translation, proteasome, protein folding/transport, and cell growth/development. The functional units of energy metabolism

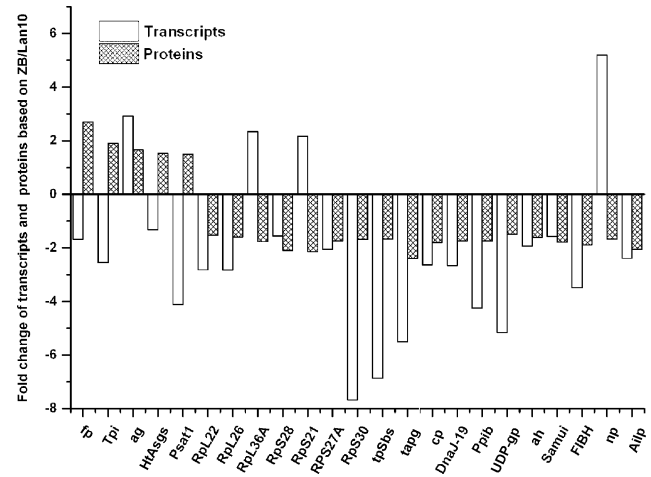


Figure 4. Correlation of the regulation patterns between transcripts and proteins based on ZB/Lan10. The y axis positive direction indicates the increased/upregulated proteins/transcripts, and the y axis negative direction indicates the decreased/downregulated proteins/transcripts.

were divided according to the pathways associated with the proteins/transcripts involved. The proteins/transcripts on the left mitochondria were associated with the Krebs cycle and those on the right were associated with the respiratory chain.

DISCUSSION

Energy Metabolism Is Vital for Silk Production

A total of 7 of the 24 proteins with increased abundance have roles in energy metabolism (Table 1), indicating that the gland of the ZB strain has higher metabolic energy demands. Dihydroliipoamide dehydrogenase, citrate synthase 1, and D-3-phosphoglycerate dehydrogenase are essential enzymes involved in glycolysis and the TCA cycle,^{22,23} and the ferritin precursor participates in iron and oxygen metabolism pathways in organisms.²⁴ In addition, NAD-dependent methylenetetrahydrofolate dehydrogenase and cytosolic 10-formyltetrahydrofolate dehydrogenase are involved in folate metabolism. Foliates play an essential role in one-carbon methyl transfer reactions and mediate several biological processes, including DNA synthesis, gene expression regulation through methylation reactions, amino acid breakdown, and thymidine and purine synthesis.²⁵ The increased energy metabolism in the ZB strain relative to that in the control strain Lan10 is consistent with a report by Wang et al.¹³ However, the fact that most of the proteins identified in this study were different from those identified in the previous study refined the proteomics. Therefore, this study expands the current knowledge of silk gland proteins and further supports the importance of energy metabolism in silk production. EGFP was most upregulated in the increased proteins because it was used as a marker gene to screen the positive transgenic silkworm, so it can only be expressed in the ZB strain. The protein that was most heavily downregulated, collagen alpha-1(IV) chain from the main segment of basement membranes,²⁶ may be one factor in the dramatically reduction of posterior silk gland cells in the ZB strain.

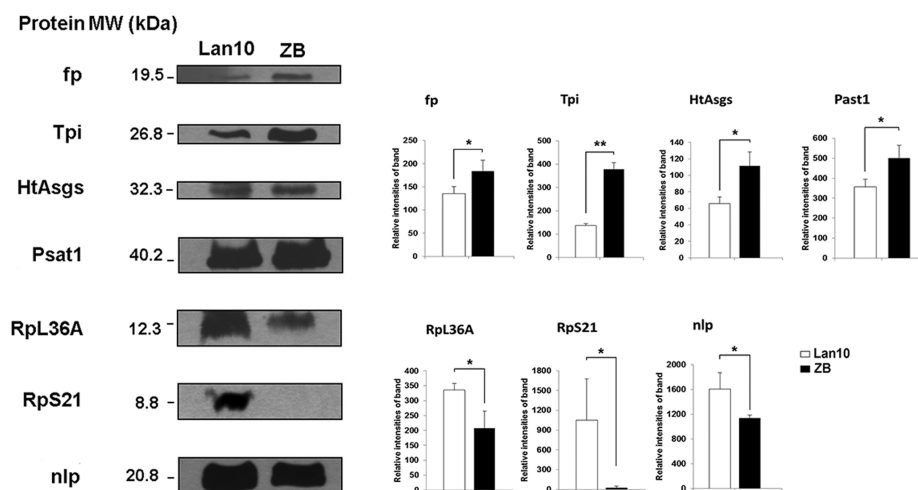


Figure 5. Identification of protein abundance of significantly changed transcripts and proteins with different regulation direction. Proteins were extracted from Lan10 and ZB and separated by SDS-polyacrylamide gel electrophoresis and transferred onto a polyvinylidene difluoride membrane. The membranes were incubated with anti-ferritin precursor (fp), anti-triosephosphate isomerase (tpi), anti-H⁺ transporting ATP synthase gamma subunit (HtAsgs), anti-phosphoserine aminotransferase 1 (Psat1), anti-RpL36A (rpL36A), anti-RpS21 (rpS21), and anti-nucleoplasmin-like protein (nlp) antibodies. Actin 3 was used as control protein. The dilution of antibodies against fp, tpi, HtAsgs, Psat1, rpL36A, rpS21, nlp, and Actin 3 were 1:1000, 1:1000, 1:5000, 1:200, 1:500, 1:1000, and 1:1000, respectively. The relative intensities of bands were calculated using ImageJ software. ** indicates that the difference in gene expression between ZB and Lan10 reached the extremely significant level, $P < 0.01$, and * indicates that the difference in gene expression between ZB and Lan10 reached a significant level, $0.01 < P < 0.05$.

Decreased Abundance Levels of Ribosomal Proteins Affect the Translational Machinery

Regarding the 65 proteins with decreased abundance (Table 1), 11 ribosomal proteins related to protein synthesis and secretion represented the majority of these proteins. rRNA plays a major role in ribosomal function, such as decoding and peptidyl-transferase activity; however, ribosomal proteins are indispensable for the assembly and optimal function of the ribosome.²⁷ RPS12 and RPL22 are involved in regulating the translational machinery,^{27,28} RPS28 is functionally important in the decoding activity of ribosomes and in the control of translational accuracy,²⁹ and RPL19 is essential for the viability of ribosomes.³⁰ Furthermore, the ribosomal proteins S12, S21, S26, S27A, S28, and S30 are important for ribosome assembly, and the ribosomal proteins L19, L22, L23A, L26, and L36A play important roles in maintaining the architectural role of the 80S ribosome.^{31,32} The abundance levels of all of the above ribosomal proteins in the ZB strain suggest that the efficiency of protein translation in ribosomes is reduced, thus hindering protein synthesis in the silk glands of the ZB strain. These results suggest that silk protein production is inevitably jeopardized in the ZB strain.

Proteins Related to Transportation and Folding Have Decreased Abundance

Most of proteins and peptides are transported to the ER or Golgi for further processing and then perform their biological functions in cells.³³ Of the six proteins associated with this process, the transport protein Sec61 beta subunit, translocation protein Sec63 homologue (DnaJ-19), TRAP gamma isoform 1, and TRAM protein are directly involved in protein transport. The Sec translocon is conserved across all organisms, and its primary components are a complex of Sec61 α , β , and γ .³⁴ Sec63 and Sec61 proteins, which are components of the translocation channel, couple with BiP, which is a member of heat shock protein 70 family present in the ER lumen.³⁵ These proteins work together to maintain proteins in a nonaggregated state for degradation or to retrieve misfolded soluble proteins from the

Golgi rather than directly targeting proteins to the retro-translocation machinery.³⁵ TRAP complex and TRAM are important accessory factors for protein transmembrane transport.³⁶ Overall, the reduced levels of these significant proteins impair protein synthesis and secretion in posterior silk gland cells of the ZB strain.

Two proteins, sarco/ER calcium ATPase and calreticulin precursor, are related to Ca²⁺ transport, which is involved in protein transportation and signal transduction.^{16,37} The loss of function of calreticulin results in the activation of ER stress, which is accompanied by a significant increase in proteasome activity. In calreticulin-deficient cells, the transcriptional activity of NF κ B significantly decreases.¹⁶ As expected, if biosynthetic activities are indeed modulated, then protein synthesis will also be affected. The decreased levels of these transport-related proteins indicate that protein transport and secretion may be reduced in the ZB strain, thus clearly reducing silk production. Protein folding is important for forming the 3D conformations of proteins and peptides before they become biologically active. Most proteins, including fibroin, must fold into defined 3D structures for their normal function. To avoid aberrant folding and aggregation of newly synthesized proteins in the cellular environment, cells invest in a complex network of molecular chaperones, which use ingenious mechanisms to prevent aggregation and to promote efficient folding.²⁶ As expected, if the folding activity of proteins has lowered abundance, then protein production should also decrease. This reasoning is consistent with our data because three proteins with decreased levels were related to protein assembly, disassembly, and translocation;^{38–40} these proteins were prefoldin beta subunit, DnaJ-19, and peptidylprolyl isomerase B precursor. This result indicates that decreased protein processing and synthesis correspond with low silk protein production in the ZB strain.

Dwarfed Growth and Development of the Posterior Silk Gland Hampers Silk Production

The growth and development of posterior silk glands is important for fibroin synthesis and secretion.⁵ The decreased

close proximity to nascent chains, enhances the translocation of some secretory proteins, and the TRAP complex is composed of four membrane protein subunits in which the γ subunit crosses the membrane four times.⁵²

The synthesis and secretion of the polymer composed of fibroin heavy chain, light chain, and P25 may be affected by this ribosome-translocation channel, and the decreased abundances of channel accessory factors, such as TRAM and TRAP gamma isoform 1, may affect protein transport. In addition, the structure of protein transport channels is closely related to the 80S ribosomal proteins, including L22, L23, and L19e.^{53,54} The decreased level of the transport protein Sec61 beta subunit, combined with the above decreased ribosomal proteins, may have negative roles in the export of polypeptides in the ZB strain. The process of ribosomal translation and peptide/protein transport involves functional machinery, which indicates that the stability of the ribosome-channel complex is essential to the production of proteins. The reduced abundances of ribosomal proteins and subunits that compose the transport channel may affect the functional stability of the entire system, resulting in low silk production in the ZB strain.

Important Functional Terms Are Implicated in Silk Production

The GO term annotation can provide functional knowledge regarding the genes and proteins in cells.⁵⁵ For the differentially expressed proteins, the most represented terms in biological and metabolic process categories indicated enhanced metabolism in the ZB strain. Ribosomal proteins are not only essential in the assembly of translational machinery but also important in the transport of primary proteins.⁵⁶ The highly represented ribosomal proteins with decreased levels in the macromolecular complex category indicate that these cellular components are functionally reduced on the third day of the fifth instar of the ZB strain. The energy metabolism and regulation of a cell are involved primarily in the catalytic activities of enzymes.²³ The highly represented catalytic activities with increased protein levels in the molecular function category also reflect the strong metabolic activity in the ZB strain. For the differentially altered transcripts, the highly represented metabolic process and catalytic activity terms signify enhanced energy metabolism. Increased levels of protein degradation indicate the coming of the cocoon period for silkworms.⁵⁷ Noticeably, 27 transcripts implicated in proteolysis are a sign of increased protein degradation levels in the ZB strain. The third day of the fifth instar is an essential time point for silk production; the earlier occurrence of protein degradation may affect the physiological state and silk production significantly. The protein species and transcripts identified here differed from a previous study, suggesting the significance of extending proteome and transcriptome knowledge regarding the silk gland.

Key Pathways of Downregulated Ribosomes and Upregulated Metabolism Affect Silk Production

The KEGG database has been used as a reference for understanding the higher-level functions of behaviors of cells or organisms from large-scale molecular data sets.⁵⁸ The wide range of pathways enriched in the present data suggests that the normal function of the posterior silk gland requires a wide repertoire of metabolic pathways (Figure 2). Most of the pathways enriched by proteins with increased levels were involved in energy metabolism, further indicating the enhanced energy demand in the ZB strain. The increased abundances of proteins with catalytic activity promoted the upregulation of

these important biological pathways that are associated with the metabolism of energy and materials *in vivo*.⁵⁹ Proteins with increased abundances were enriched in the pathways of glycine, serine, and threonine metabolism, suggesting highly induced activity in these pathways. Glycine and serine account for 40 and 12% of the amino acid composition of fibroin heavy chain;⁶⁰ however, the functionally increased pathway of amino acid metabolism in the ZB strain may not play a positive role in promoting silk protein production.

In contrast, the lowered silk production in the ZB strain may result from the inefficient application of amino acids during silk production. In addition, supplying amino acids is only the first step in protein synthesis; the subsequent post-translational modifications of proteins, protein processing in the ER, transport, and extracellular secretion are all essential to protein production.^{61,62} The weakened functions of proteins in the above processes linked to the BIN may be the primary reason for the low efficiency of protein synthesis in the ZB strain. However, in addition to their roles as components of protein synthesis, several amino acids have other functions. For example, levels of glycine increase because of deficiencies of the glycine cleavage enzyme, and the increased levels enzymes phosphoglycerate dehydrogenase and phosphoserine aminotransferase may be used to synthesize endogenous serine.²⁵

For the pathways enriched by proteins with decreased abundance levels, the most abundant protein is the ribosome (Supporting Information Figure 4). A large number of ribosome proteins in the nucleus that were linked to the BIN decreased their abundance levels; these decreases play a negative role in ribosome assembly and reduce the activity of the ribosome pathway.⁶³ The proteins with decreased abundance levels that were enriched in the pathway of protein processing in the ER were also highly represented (Supporting Information Figure 5), indicating that the processing and transport of proteins in the ER may be weakened in the ZB strain. Protein processing in the ER is an extremely important step for the post-translational modification of proteins, which is closely related to the subsequent transport and secretion of proteins.⁶⁴ The reduced pathways functioning in the ribosome transport channel in the ZB strain indicate their roles in impairing protein synthesis and secretion. Another pathway, spliceosome (Supporting Information Figure 6), which is involved at the transcriptional level, was mapped to proteins with decreased abundances. Eukaryotic mRNAs experience complex lives from birth to death, during which post-transcriptional modification controls gene expression.⁶⁵ Pre-mRNA splicing and transportation are the primary steps for post-transcriptional modification. The spliceosome is a complex macromolecular machinery that catalyzes pre-mRNA splicing,⁶⁶ which is a vital step for post-transcriptional regulation. These results suggest that the decreased function of the spliceosome pathway may decrease the splicing accuracy in the pre-mRNA, which will affect the normal expression of related genes, particularly fibroin- and fibroin-yield-related genes.

The transcripts and proteins from the previous and present studies are summarized in Figure 6. Five primary regulatory functions, energy metabolism, proteasome, transcription/translation, protein folding/transport, and cell growth/development, were affected in the mutated strain ZB. This figure therefore gives a comprehensive view of the molecular mechanisms underlying low silk production.

Identifying Novel Transcripts Extends the Understanding of Silk Production

The transcript data set used in the present study offers a complementary result to our previous experiment.¹³ Most energy metabolism-related transcripts were identified by both RNA sequencing experiments (Supporting Information Table 8). Noticeably, most transcripts in the present study were involved in metabolic pathways, whereas the energy metabolism-related transcripts were involved primarily in the oxidative phosphorylation pathway in our previous study, providing a stronger indication that the inefficient energy utilization in the ZB strain may be an important reason for its low silk production. Although the transcripts related to proteolysis (GO: 0006508) were also found in both studies (Supporting Information Table 9), only 7 transcripts were identified previously, whereas 21 were identified in the present study, indicating an expansion of transcriptome coverage in this pathway and its biological importance. The stronger functional proteasome pathway,¹³ together with increased proteolysis in the ZB strain, may affect silk production significantly because of accelerated cell apoptosis⁶⁷ or impair the function of protein transportation,⁶⁸ particularly at the time point of the third day of the fifth instar when silk production is rapid and abundant.

Abundance Levels of Proteins and Transcripts Related to Fibroin Synthesis Are Highly Consistent

The proteomic results underscored the importance of the synthesis and secretion of regulatory proteins. qRT-PCR validated the expression levels of the corresponding transcripts (Figure 3). Post-transcriptional regulation is common and important in gene expression.⁶⁹ Therefore, not all the transcript expression levels were consistent with the protein abundances (Figure 4). The relationship between gene expression at the transcriptional level and the level of translation is not always consistent because of post-translational modifications and splicing events in cells.⁶⁹ The Western blot analysis of the proteins with up- or downregulated transcripts showed the same abundance trends as the proteomic analysis, which strongly supports our conclusions (Figure 5). The primary component of fibroin, which is fibroin heavy chain, was decreased at both the transcriptional and translational levels. The fibroin heavy chain, fibroin light chain, and P25 proteins form the elementary unit of fibroin, which consists of a 6:6:1 molar ratio of H-chain/L-chain/P25.⁷⁰ The decreased abundance of fibroin heavy chain may be one of the reasons for the thin cocoon structure observed in the ZB strain. In the future, a gene knockout experiment may be performed to verify this interpretation. Together, the ribosome function, protein folding, processing, and transport, posterior silk gland growth and development, and protein synthesis and secretion in the ZB strain will be weakened.

CONCLUSIONS

Silk production in silkworms is a typical complex trait that is controlled by multiple genes. The present study found four important molecular mechanisms underlying the low silk production observed in the ZB strain: (i) The decreased abundance of proteins associated with cell growth/development results in the reduced growth/development of the posterior silk gland of the silkworm. (ii) The inefficient application of energy metabolism in silk production and decreased transcriptional activity impair the expression of genes related to fibroin synthesis, such as the silk fibroin heavy

chain. (iii) The decreased levels of ribosomal proteins, proteins for protein folding, and the proteins related to fibroin transport in the ER and Golgi body affect the normal synthesis, folding and transport of fibroin. (iv) The increased proteasome and ubiquitin expression increase the rate of protein degradation.

ASSOCIATED CONTENT

Supporting Information

The Supporting Information is available free of charge on the ACS Publications website at DOI: 10.1021/acs.jproteome.5b00821.

Error distribution of the relative molecular weights of all the mapped peptides. Biological interaction network for differentially altered proteins between ZB and Lan10. Differentially altered proteins involved in protein synthesis and secretion. Pathway of the ribosome. Pathway of protein processing in the ER. Pathway of the spliceosome. (PDF)

Primer sequences used for qRT-PCR of differentially expressed genes between ZB and Lan10 in the posterior silk gland of the silkworm on day 3 of the fifth instar. (XLSX)

Total number of proteins identified from the posterior silk gland of the silkworm on day 3 of the fifth instar using the iTRAQ proteomic technique. (XLSX)

Detailed information on differentially altered transcripts with new exons between ZB and Lan10 in the posterior silk gland of the silkworm on day 3 of the fifth instar. (XLS)

Pathways enrich by differentially changed proteins/transcripts between ZB and Lan10 in the posterior silk gland of the silkworm on day 3 of the fifth instar. (XLSX) Full names and abbreviations of proteins in Figures 3–6 and Supporting Information Figure 3. (XLSX)

Differentially altered proteins between ZB and Lan10 in the BIN. (XLS)

GO analysis of the differentially altered transcripts between ZB and Lan10 in the posterior silk gland of the silkworm on day 3 of the fifth instar. (XLSX)

Upregulated transcripts involved in energy metabolism in the previous study and in the present study. (XLSX)

Upregulated transcripts involved in the GO term proteolysis in the previous study and in the present study. (XLSX)

AUTHOR INFORMATION

Corresponding Author

*Tel.: +86-571-86971302. E-mail: bxzhong@zju.edu.cn.

Author Contributions

S.W. and Z.Y. contributed equally to this work.

Funding

This work was supported by the National Basic Research Program of China (grant no. 2012CB114601) for Z.B.X.

Notes

The authors declare no competing financial interest.

REFERENCES

- (1) International Silkworm Genome Consortium. The genome of a lepidopteran model insect, the silkworm *Bombyx mori*. *Insect Biochem. Mol. Biol.* **2008**, *38*, 1036–1045.

- (2) Goldsmith, M. R.; Shimada, T.; Abe, H. The genetics and genomics of the silkworm, *Bombyx mori*. *Annu. Rev. Entomol.* **2005**, *50*, 71–100.
- (3) Nagano, A.; Tanioka, Y.; Sakurai, N.; Sezutsu, H.; Kuboyama, N.; Kiba, H.; Tanimoto, Y.; Nishiyama, N.; Asakura, T. Regeneration of the femoral epicondyle on calcium-binding silk scaffolds developed using transgenic silk fibroin produced by transgenic silkworm. *Acta Biomater.* **2011**, *7*, 1192–201.
- (4) Hofmann, S.; Hagenmuller, H.; Koch, A. M.; Muller, R.; Vunjak-Novakovic, G.; Kaplan, D. L.; Merkle, H. P.; Meinel, L. Control of in vitro tissue-engineered bone-like structures using human mesenchymal stem cells and porous silk scaffolds. *Biomaterials* **2007**, *28*, 1152–62.
- (5) Hou, Y.; Xia, Q.; Zhao, P.; Zou, Y.; Liu, H.; Guan, J.; Gong, J.; Xiang, Z. Studies on middle and posterior silk glands of silkworm (*Bombyx mori*) using two-dimensional electrophoresis and mass spectrometry. *Insect Biochem. Mol. Biol.* **2007**, *37*, 486–96.
- (6) Li, J.; Ye, L.; Lan, T.; Yu, M.; Liang, J.; Zhong, B. Comparative proteomic and phosphoproteomic analysis of the silkworm (*Bombyx mori*) posterior silk gland under high temperature treatment. *Mol. Biol. Rep.* **2012**, *39*, 8447–56.
- (7) Li, J.; Yang, H.; Lan, T.; Wei, H.; Zhang, H.; Chen, M.; Fan, W.; Ma, Y.; Zhong, B. Expression profiling and regulation of genes related to silkworm posterior silk gland development and fibroin synthesis. *J. Proteome Res.* **2011**, *10*, 3551–64.
- (8) Li, J.; Cai, Y.; Ye, L.; Wang, S.; Che, J.; You, Z.; Yu, J.; Zhong, B. MicroRNA expression profiling of the fifth-instar posterior silk gland of *Bombyx mori*. *BMC Genomics* **2014**, *15*, 410.
- (9) Ma, L.; Xu, H.; Zhu, J.; Ma, S.; Liu, Y.; Jiang, R. J.; Xia, Q.; Li, S. Ras1CA overexpression in the posterior silk gland improves silk yield. *Cell Res.* **2011**, *21*, 934–43.
- (10) Medin, J. A.; Hunt, L.; Gathy, K.; Evans, R. K.; Coleman, M. S. Efficient, low-cost protein factories: expression of human adenosine deaminase in baculovirus-infected insect larvae. *Proc. Natl. Acad. Sci. U. S. A.* **1990**, *87*, 2760–2764.
- (11) Takei, F.; Oyama, F.; Kimura, K.; Hyodo, A.; Mizuno, S.; Shimura, K. Reduced level of secretion and absence of subunit combination for the fibroin synthesized by a mutant silkworm, Nd(2). *J. Cell Biol.* **1984**, *99*, 2005–10.
- (12) Inoue, S.; Kanda, T.; Imamura, M.; Quan, G. X.; Kojima, K.; Tanaka, H.; Tomita, M.; Hino, R.; Yoshizato, K.; Mizuno, S. A fibroin secretion-deficient silkworm mutant, Nd-sD, provides an efficient system for producing recombinant proteins. *Insect Biochem. Mol. Biol.* **2005**, *35*, 51–59.
- (13) Wang, S.; You, Z.; Ye, L.; Che, J.; Qian, Q.; Nanjo, Y.; Komatsu, S.; Zhong, B. Quantitative proteomic and transcriptomic analyses of molecular mechanisms associated with low silk production in silkworm *Bombyx mori*. *J. Proteome Res.* **2014**, *13*, 735–51.
- (14) Zhou, Z.; Yang, H.; Chen, M.; Lou, C.; Zhang, Y.; Chen, K.; Wang, Y.; Yu, M.; Yu, F.; Li, J.; Zhong, B.-x. Comparative proteomic analysis between the domesticated silkworm (*Bombyx mori*) reared on fresh mulberry leaves and on artificial diet. *J. Proteome Res.* **2008**, *7*, 5103–5111.
- (15) Unwin, R. D.; Griffiths, J. R.; Whetton, A. D. Simultaneous analysis of relative protein expression levels across multiple samples using iTRAQ isobaric tags with 2D nano LC-MS/MS. *Nat. Protoc.* **2010**, *5*, 1574–82.
- (16) Walker, J. M. The bicinechonic acid (BCA) assay for protein quantitation. *Methods Mol. Biol.* **1994**, *32*, 5–8.
- (17) Ye, J.; Fang, L.; Zheng, H.; Zhang, Y.; Chen, J.; Zhang, Z.; Wang, J.; Li, S.; Li, R.; Bolund, L.; Wang, J. WEGO: a web tool for plotting GO annotations. *Nucleic Acids Res.* **2006**, *34*, W293–W297.
- (18) Nikitin, A.; Egorov, S.; Daraselia, N.; Mazo, I. Pathway studio-the analysis and navigation of molecular networks. *Bioinformatics* **2003**, *19*, 2155–57.
- (19) Kanehisa, M.; Goto, S. KEGG: kyoto encyclopedia of genes and genomes. *Nucleic Acid Res.* **2000**, *28*, 27–30.
- (20) Ramakrishnan, V. Ribosome structure and the mechanism of translation. *Cell* **2002**, *108*, 557–72.
- (21) Asakura, T.; Tanaka, C.; Yang, M.; Yao, J.; Kurokawa, M. Production and characterization of a silk-like hybrid protein, based on the polyalanine region of *Samia cynthia ricini* silk fibroin and a cell adhesive region derived from fibronectin. *Biomaterials* **2004**, *25*, 617–24.
- (22) Fernie, A. R.; Carrari, F.; Sweetlove, L. J. Respiratory metabolism: glycolysis, the TCA cycle and mitochondrial electron transport. *Curr. Opin. Plant Biol.* **2004**, *7*, 254–61.
- (23) Atkinson, D. E. *Cellular energy metabolism and its regulation*. Academic Press: New York, 1977.
- (24) Theil, E. C. Ferritin: at the crossroads of iron and oxygen metabolism. *J. Nutr.* **2003**, *133*, 1549S–1553S.
- (25) Scaglia, F.; Blau, N. Disorders of folate metabolism and transport. In *Physician's Guide to the Diagnosis, Treatment, and Follow-Up of Inherited Metabolic Diseases*; Blau, N., Duran, M., Gibson, K. M., Vici, C. D., Eds.; Springer: Berlin Heidelberg, 2014; pp 167–178.
- (26) Glanville, R. W. Type IV collagen. *Structure and function of collagen types* **1987**, 43–79.
- (27) Wilson, D. N.; Nierhaus, K. H. Ribosomal proteins in the spotlight. *Crit. Rev. Biochem. Mol. Biol.* **2005**, *40*, 243–67.
- (28) Tabb-Massey, A.; Caffrey, J. M.; Logsdon, P.; Taylor, S.; Trent, J. O.; Ellis, S. R. Ribosomal proteins Rps0 and Rps21 of *Saccharomyces cerevisiae* have overlapping functions in the maturation of the 3' end of 18S rRNA. *Nucleic Acid Res.* **2003**, *31*, 6798–6805.
- (29) Synetos, D.; Frantziou, C. P.; Alksne, L. E. Mutations in yeast ribosomal proteins S28 and S4 affect the accuracy of translation and alter the sensitivity of the ribosomes to paromomycin. *Biochim. Biophys. Acta, Gene Struct. Expression* **1996**, *1309*, 156–66.
- (30) Dresios, J.; Panopoulos, P.; Synetos, D. Eukaryotic ribosomal proteins lacking a eubacterial counterpart: important players in ribosomal function. *Mol. Microbiol.* **2006**, *59*, 1651–63.
- (31) Ben-Shem, A.; Garreau de Loubresse, N. G.; Melnikov, S.; Jenner, L.; Yusupova, G.; Yusupov, M. The structure of the eukaryotic ribosome at 3.0 Å resolution. *Science* **2011**, *334*, 1524–1529.
- (32) Taylor, D. J.; Devkota, B.; Huang, A. D.; Topf, M.; Narayanan, E.; Sali, A.; Harvey, S. C.; Frank, J. Comprehensive molecular structure of the eukaryotic ribosome. *Structure* **2009**, *17*, 1591–604.
- (33) Krieg, U. C.; Johnson, A. E.; Walter, P. Protein translocation across the endoplasmic reticulum membrane: identification by photocross-linking of a 39-kD integral membrane glycoprotein as part of a putative translocation tunnel. *J. Cell Biol.* **1989**, *109*, 2033–2043.
- (34) Du Plessis, D. J.; Nouwen, N.; Driessen, A. J. The sec translocase. *Biochim. Biophys. Acta, Biomembr.* **2011**, *1808*, 851–65.
- (35) Tsai, B.; Ye, Y.; Rapoport, T. A. Retro-translocation of proteins from the endoplasmic reticulum into the cytosol. *Nat. Rev. Mol. Cell Biol.* **2002**, *3*, 246–55.
- (36) Shao, S.; Hegde, R. S. Membrane protein insertion at the endoplasmic reticulum. *Annu. Rev. Cell Dev. Biol.* **2011**, *27*, 25–56.
- (37) Manjarrés, I. M.; Rodríguez-García, A.; Alonso, M. T.; García-Sancho, J. The sarco/endoplasmic reticulum Ca²⁺-ATPase (SERCA) is the third element in capacitative calcium entry. *Cell Calcium* **2010**, *47*, 412–18.
- (38) Sahlan, M.; Zako, T.; Tai, P. T.; Ohtaki, A.; Noguchi, K.; Maeda, M.; Miyatake, H.; Dohmae, N.; Yohda, M. Thermodynamic characterization of the interaction between prefoldin and group II chaperonin. *J. Mol. Biol.* **2010**, *399*, 628–36.
- (39) Walsh, P.; Bursac, D.; Law, Y. C.; Cyr, D.; Lithgow, T. The J-protein family: modulating protein assembly, disassembly and translocation. *EMBO Rep.* **2004**, *5*, 567–71.
- (40) Xia, H.; Lv, H.; Chen, K.; Yao, Q.; Lv, P.; Li, J.; Chen, H.; Wang, L. Cloning and characterization of peptidylprolyl isomerase B in the silkworm, *Bombyx mori*. *Afr. J. Biotechnol.* **2009**, *8*, 7116–7124.
- (41) Saito, Y.; Shibayama, H.; Tanaka, H.; Tanimura, A.; Kanakura, Y. A cell-death-defying factor, anamorsin mediates cell growth through inactivation of PKC and p38MAPK. *Biochem. Biophys. Res. Commun.* **2011**, *405*, 303–7.
- (42) Shikata, M.; Shibata, H.; Sakurai, M.; Sano, Y.; Hashimoto, Y.; Matsumoto, T. The ecdysteroid UDP-glucosyltransferase gene of

Autographa californica nucleopolyhedrovirus alters the moulting and metamorphosis of a non-target insect, the silkworm, *Bombyx mori* (Lepidoptera, Bombycidae). *J. Gen. Virol.* **1998**, *79*, 1547–1551.

(43) Doong, H.; Vrailas, A.; Kohn, E. C. What's in the 'BAG'?—a functional domain analysis of the BAG-family proteins. *Cancer Lett.* **2002**, *188*, 25–32.

(44) Moribe, Y.; Niimi, T.; Yamashita, O.; Yaginuma, T. Samui, a novel cold-inducible gene, encoding a protein with a BAG domain similar to silencer of death domains (SODD/BAG-4), isolated from *Bombyx* diapause eggs. *Eur. J. Biochem.* **2001**, *268*, 3432–42.

(45) Irvine, K. D. A notch sweeter. *Cell* **2008**, *132*, 177–79.

(46) Gumbart, J.; Trabuco, L. G.; Schreiner, E.; Villa, E.; Schulten, K. Regulation of the protein-conducting channel by a bound ribosome. *Structure* **2009**, *17*, 1453–64.

(47) Spahn, C. M.; Beckmann, R.; Eswar, N.; Penczek, P. A.; Sali, A.; Blobel, G.; Frank, J. Structure of the 80S ribosome from *Saccharomyces cerevisiae*-tRNA-ribosome and subunit-subunit interactions. *Cell* **2001**, *107*, 373–86.

(48) Mitra, K.; Frank, J. A model for co-translational translocation: ribosome-regulated nascent polypeptide translocation at the protein-conducting channel. *FEBS Lett.* **2006**, *580*, 3353–60.

(49) Becker, T.; Bhushan, S.; Jarasch, A.; Armache, J.-P.; Funes, S.; Jossinet, F.; Gumbart, J.; Mielke, T.; Berninghausen, O.; Schulten, K.; et al. Structure of monomeric yeast and mammalian Sec61 complexes interacting with the translating ribosome. *Science* **2009**, *326*, 1369–1373.

(50) Park, E.; Ménétret, J.-F.; Gumbart, J. C.; Ludtke, S. J.; Li, W.; Whynot, A.; Rapoport, T. A.; Akey, C. W. Structure of the SecY channel during initiation of protein translocation. *Nature* **2013**, *506*, 102.

(51) Daniel, C. J.; Conti, B.; Johnson, A. E.; Skach, W. R. Control of translocation through the Sec61 translocon by nascent polypeptide structure within the ribosome. *J. Biol. Chem.* **2008**, *283*, 20864–73.

(52) Menetret, J.-F.; Hegde, R. S.; Heinrich, S. U.; Chandramouli, P.; Ludtke, S. J.; Rapoport, T. A.; Akey, C. W. Architecture of the ribosome-channel complex derived from native membranes. *J. Mol. Biol.* **2005**, *348*, 445–57.

(53) Klein, D.; Moore, P.; Steitz, T. The roles of ribosomal proteins in the structure assembly, and evolution of the large ribosomal subunit. *J. Mol. Biol.* **2004**, *340*, 141–77.

(54) Beckmann, R.; Spahn, C. M.; Eswar, N.; Helmers, J.; Penczek, P. A.; Sali, A.; Frank, J.; Blobel, G. Architecture of the protein-conducting channel associated with the translating 80S ribosome. *Cell* **2001**, *107*, 361–72.

(55) Harris, M.; Clark, J.; Ireland, A.; Lomax, J.; Ashburner, M.; Foulger, R.; Eilbeck, K.; Lewis, S.; Marshall, B.; Mungall, C. The Gene Ontology (GO) database and informatics resource. *Nucleic Acid Res.* **2004**, *32*, D258–D261.

(56) Delaunay, J.; Mathieu, C.; Schapira, G. Eukaryotic ribosomal proteins. *Eur. J. Biochem.* **1972**, *31*, 561–64.

(57) Matsuura, S.; Morimoto, T.; Nagata, S.; Tashiro, Y. Studies on the posterior silk gland of the silkworm, *Bombyx mori* II. Cytolytic processes in posterior silk gland cells during metamorphosis from larva to pupa. *J. Cell Biol.* **1968**, *38*, 589–603.

(58) Kanehisa, M.; Araki, M.; Goto, S.; Hattori, M.; Hirakawa, M.; Itoh, M.; Katayama, T.; Kawashima, S.; Okuda, S.; Tokimatsu, T.; Yamanishi, Y. KEGG for linking genomes to life and the environment. *Nucleic Acids Res.* **2007**, *36*, D480–D484.

(59) Jahic, M.; Rotticci-Mulder, J.; Martinelle, M.; Hult, K.; Enfors, S.-O. Modeling of growth and energy metabolism of *Pichia pastoris* producing a fusion protein. *Bioprocess Biosyst. Eng.* **2002**, *24*, 385–393.

(60) Zhou, C.-Z.; Confalonieri, F.; Medina, N.; Zivanovic, Y.; Esnault, C.; Yang, T.; Jacquet, M.; Janin, J.; Duguet, M.; Perasso, R. Fine organization of *Bombyx mori* fibroin heavy chain gene. *Nucleic Acids Res.* **2000**, *28*, 2413–2419.

(61) Kojima, K.; Kuwana, Y.; Sezutsu, H.; Kobayashi, I.; Uchino, K.; Tamura, T.; Tamada, Y. A New Method for the Modification of Fibroin Heavy Chain Protein in the Transgenic Silkworm. *Biosci., Biotechnol., Biochem.* **2007**, *71*, 2943–51.

(62) Kelly, R. B. Pathways of protein secretion in eukaryotes. *Science* **1985**, *230*, 25–32.

(63) Hershey, J. W.; Merrick, W. C. Pathway and mechanism of initiation of protein synthesis. *Cold Spring Harbor Monogr. Ser.* **2000**, *39*, 33–88.

(64) Pelham, H. R. Control of protein exit from the endoplasmic reticulum. *Annu. Rev. Cell Biol.* **1989**, *5*, 1–23.

(65) Moore, M. J.; Schwartzfarb, E. M.; Silver, P. A.; Yu, M. C. Differential recruitment of the splicing machinery during transcription predicts genome-wide patterns of mRNA splicing. *Mol. Cell* **2006**, *24*, 903–15.

(66) Will, C. L.; Lührmann, R. Spliceosomal UsnRNP biogenesis, structure and function. *Curr. Opin. Cell Biol.* **2001**, *13*, 290–301.

(67) Kidd, V. J. Proteolytic activities that mediate apoptosis. *Annu. Rev. Physiol.* **1998**, *60*, 533–73.

(68) Wyllie, A. H.; Kerr, J. R.; Currie, A. Cell death: the significance of apoptosis. *Int. Rev. Cytol.* **1980**, *68*, 251–306.

(69) Pandey, A.; Mann, M. Proteomics to study genes and genomes. *Nature* **2000**, *405*, 837–846.

(70) Inoue, S.; Kanda, T.; Imamura, M.; Quan, G.; Kojima, K.; Tanaka, H.; Tomita, M.; Hino, R.; Yoshizato, K.; Mizuno, S. A fibroin secretion-deficient silkworm mutant, provides an efficient system for producing recombinant proteins. *Insect Biochem. Mol. Biol.* **2005**, *35*, 51–59.